Convection in a saturated porous medium at large Rayleigh number or Péclet number

By R. A. WOODING

Applied Mathematics Laboratory, D.S.I.R., Wellington, New Zealand

(Received 18 June 1962 and in revised form 23 October 1962)

When the dimensions of a convective system in a saturated porous medium are sufficiently great, diffusion effects can be neglected except in regions where the gradients of fluid properties are very large. A boundary-layer theory is developed for vertical plane flows in such regions. In special cases, the theory is equivalent to that for laminar incompressible flow in a two-dimensional half-jet, or in a plane jet or round jet, for which similarity solutions are well known.

A number of experiments have been performed using a Hele–Shaw cell immersed in water, with a source of potassium permanganate solution located between the plates. At very small values of the source strength, a flow analogous to that of a plane jet from a slit is obtained. The distance advanced by the jet front, or cap, is measured as a function of time, and the velocity is found to be nearly proportional to the velocity of the fluid on the axis of the steady jet behind the cap, as given by the similarity law of Schlichting and Bickley. At large values of the source strength, a two-dimensional 'broad jet' of homogeneous solution descending under gravity is produced; the shape of the flow region can be calculated with little error from potential theory, neglecting the effect of the mixing layers.

A possible example of a mixing layer observed in a geothermal region is examined. The theoretical form of the temperature distribution is calculated numerically, taking into account the large viscosity variation with temperature and also the possibility of a large permeability variation. These effects are found to have less influence upon the solution than might have been expected. Quantitative values obtained for the physical parameters are consistent with other geophysical observations.

1. Introduction

In the steady motion of ground water under non-isothermal conditions, or of ground water with other non-homogeneous physical properties, the macroscopic length scale of the system may be so great that diffusion effects can be considered negligible. An approximation of this type was made by Yih (1961) who showed that, in the absence of differential buoyancy effects, the flow problem for a non-homogeneous fluid could be transformed into an equivalent potential problem for a homogeneous fluid. Yih also obtained solutions by inverse methods for two-dimensional flows which included significant buoyancy effects.

This paper is concerned with the properties of steady vertical convection from a source of heat or of heated fluid in a saturated porous medium when the Rayleigh number or the Péclet number exceeds $O(10)$. The effects of thermal diffusion are important only in zones of mixing between fluids at different temperatures, and here the nature of the fluid motion is such that boundary-layer approximations are valid. Flows of this type might be found in geothermal areas, or might arise from the heat generated by deep explosions in saturated ground.

The treatment will be limited to two-dimensional flows, taking the flow-plane (x, y) vertical, with the x-axis directed vertically upwards. The medium will be assumed isotropic, with constant porosity, but in certain cases the permeability may vary with temperature. Let the fluid be incompressible, changing volume only as a result of changes in temperature; from the Boussinesq approximation,

$$(\rho - \rho_0)/\rho_0 = -\alpha(T - T_0)/T_0, \tag{1}$$

where ρ and T are the density and Absolute temperature, ρ_0 is the density at a reference temperature T_0, and α is a constant. The components of the flow-vector in the x- and y-directions will be designated u^* and v^*; however, it is convenient to introduce a 'modified flow vector' (u, v) which is defined by the relation $(\rho_0 u, \rho_0 v) = (\rho u^*, \rho v^*)$. Then the steady-state equations of continuity, motion (Darcy's law) and heat transport become

$$\frac{\partial u}{\partial x} + \frac{\partial v}{\partial y} = 0, \tag{2}$$

$$\begin{cases} \dfrac{1}{\rho_0}\dfrac{\partial P}{\partial x} + \dfrac{\nu}{k}u = -g\dfrac{\rho}{\rho_0}, & (3) \\ \dfrac{1}{\rho_0}\dfrac{\partial P}{\partial y} + \dfrac{\nu}{k}v = 0, & (4) \end{cases}$$

$$u\frac{\partial T}{\partial x} + v\frac{\partial T}{\partial y} = \frac{\partial}{\partial x}\left(\kappa_l \frac{\partial T}{\partial x}\right) + \frac{\partial}{\partial y}\left(\kappa_t \frac{\partial T}{\partial y}\right), \tag{5}$$

where k is the permeability, $\nu \equiv \nu(T)$ is the kinematic viscosity, P is the pressure, and g is the acceleration due to gravity. In equation (5), the longitudinal and transverse diffusivities κ_l and κ_t are defined by $\kappa_l = K_l/\rho_0 c$ and $\kappa_t = K_t/\rho_0 c$, where c is the specific heat of the incompressible fluid and K_l and K_t are coefficients involving the thermal conductivity of the saturated medium combined with the effects of longitudinal and transverse mechanical dispersion.

The above equations hold also for an isothermal fluid containing dissolved material, provided that T represents the concentration of solute, (u, v) is identical with (u^*, v^*) (i.e. fluid dilatation effects are negligible), κ_l and κ_t are the longitudinal and transverse components of the effective diffusivity of solute through the fluid saturating the porous medium, and provided that ν is replaced by μ/ρ_0, where μ is the dynamic viscosity.

For this latter case, the work of Saffman (1960) shows that equation (5) is valid when the Péclet number of the flow, based upon pore size and molecular diffusivity, does not exceed $O(1)$; the effect of transverse dispersion is then

small. In the present paper, it will be assumed that a similar approximation can be made for the non-isothermal problem, where the Péclet number is defined in terms of pore size and the thermal diffusivity of the saturated medium. The Péclet number will then be taken small, so that κ_t can be replaced in (5) by the thermal (or effective molecular) diffusivity κ, which is assumed constant.

2. Equations of the flow at a mixing layer

The geometrical parameters of a simplified mixing-layer problem are defined as shown in figure 1. Two impermeable and thermally-insulating partitions AC and BD, spaced a distance $2d$ apart, separate a heated fluid 1, of uniform temperature T_1', from a fluid 0, of uniform temperature T_0'. It is assumed that the motion is due only to buoyancy effects and a uniform externally applied vertical pressure gradient (implying that horizontal boundaries exist above and below the region of interest), so that the flow-rate vectors of magnitudes U_1 and U_0 are vertical.

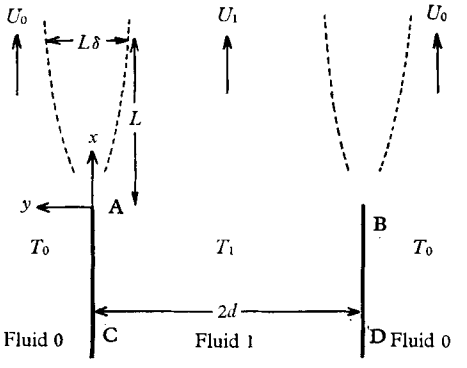

FIGURE 1. Formation of plane mixing layers between a fluid 1, of temperature T_1', which is rising with a flow rate U_1 through a fluid 0 of temperature T_0' and vertical flow rate U_0.

For each of the 'thin' mixing layers above the points A and B in figure 1, the length scales in the x- and y-directions can be taken to be $O(L)$ and $O(L\delta)$, where $\delta^2 \ll 1$. From the equation of continuity (2), $v/u = O(\delta)$; hence (4) can be integrated approximately to give

$$(P-P_0)/\rho_0 = O(\nu u L\delta^2/k), \tag{6}$$

where P_0, the pressure in fluid 0, satisfies the equation

$$\frac{1}{\rho_0}\frac{dP_0}{dx} = -\frac{\nu}{k}U_0 - g. \tag{7}$$

Equation (6) provides a measure of the total pressure change in passing through the mixing layer from fluid 0 to fluid 1.

If (1), (3), (6) and (7) are now combined to eliminate P, P_0 and $(\rho-\rho_0)/\rho_0$, there results

$$\sigma u\{1+O(\delta^2)\} = U_0 + (k_0 g\alpha/\nu_0)(T-T_0')/T_0', \tag{8}$$

where

$$\sigma = \frac{\nu}{k}\Big/\frac{\nu_0}{k_0}. \tag{9}$$

Thus the equations of motion (3) and (4) may be replaced by the approximate equation (8), neglecting the small term of order δ^2.

As a further consequence of the boundary-layer assumption, the transport equation (5) can be replaced by

$$u\partial T/\partial x + v\partial T/\partial y = \kappa \partial^2 T/\partial y^2 \tag{10}$$

provided that the ratio $\delta^2\kappa_l/\kappa \ll 1$. Elimination of T between (8) and (10) gives the equation

$$(u\partial/\partial x + v\partial/\partial y)(\sigma u) = \kappa \partial^2(\sigma u)/\partial y^2, \tag{11}$$

which is to be solved in conjunction with the equation of continuity (2) and a relation for σ, which is assumed known. From figure 1, the boundary conditions for the system are

$$u(x, \infty) = U_0, \quad u(x, -\infty) = U_1 = \frac{1}{\sigma_1}\left(U_0 + \frac{k_0 g\alpha}{\nu_0}\frac{T_1 - T_0}{T_0}\right), \tag{12}$$

using (8).

A two-dimensional stream-function ψ can be defined from (2) in the usual way.

$$u = \partial\psi/\partial y, \quad v = -\partial\psi/\partial x. \tag{13}$$

Then the transformation of von Mises (1927) can be applied to (11), giving

$$\frac{\partial}{\partial x}(\sigma u) = \kappa\frac{\partial}{\partial\psi}\left\{u\frac{\partial(\sigma u)}{\partial\psi}\right\}, \quad \text{with} \quad y = \int\frac{d\psi}{u}. \tag{14}$$

In § 5, some use is made of the equations (14) to obtain numerical solutions of a mixing-layer problem.

Conditions for the validity of the approximations

Since the terms on both sides of equation (10) must be of the same order of magnitude in the mixing layer, it is necessary that

$$\kappa/L^2\delta^2 = O(U_1/L), \quad \text{i.e.} \quad \delta = O(\kappa/U_1 L)^{\frac{1}{2}}. \tag{15}$$

The velocity scale is here defined in terms of U_1, assuming that $U_1 > U_0 \geqslant 0$, since the motion relative to the fixed points A and B (figure 1) is being considered. When the condition $\delta^2 \ll 1$ is applied to (15), using (12) to eliminate U_1, the result is

$$\frac{1}{\delta^2} = O\left(\left|\frac{k_1 g\alpha}{\nu_1\kappa}\frac{T_1 - T_0}{T_0}L + \frac{U_0 L}{\sigma_1\kappa}\right|\right) \gg 1. \tag{16}$$

A necessary condition for the boundary conditions (12) to hold is that both U_1 and U_0 should remain constant for all x. From figure 1, this condition can be satisfied provided that the two mixing layers do not merge together, i.e. provided that $d > L\delta$. This gives

$$\left|\frac{k_1 g\alpha}{\nu_1\kappa}\frac{T_1 - T_0}{T_0}\frac{d^2}{L} + \frac{U_0}{\sigma_1\kappa}\frac{d^2}{L}\right| > 1. \tag{17}$$

If L is increased indefinitely, condition (17) must ultimately fail to hold; the mixing layers begin to merge, and the distributions of temperature and velocity approach those due to a point source of heat (cf. § 3).

In each of the conditions (16) and (17), the quantity within the modulus consists of two terms, the first defining a Rayleigh number and the second a Péclet number. The two Rayleigh numbers

$$\lambda = \frac{k_1 g\alpha}{\nu_1 \kappa}\frac{T_1 - T_0}{T_0}L \quad \text{and} \quad \lambda' = \frac{k_1 g\alpha}{\nu_1 \kappa}\frac{T_1 - T_0}{T_0}\frac{d^2}{L} \tag{16', 17'}$$

are associated with free convection of fluid 1 through fluid 0, while the Péclet numbers are associated with wake-like flows due to the forced convection of the entire body of fluid under an applied vertical pressure gradient.

3. Solutions for vertical flows

Two special situations can arise in which the variable quantity σ, defined in (9), can be taken identically equal to 1. First, the permeability k may be a linear function of the kinematic viscosity ν, where ν varies with temperature; this case could be of geophysical significance (§ 5). Secondly, variations in k and ν may be small enough to be neglected.

When $\sigma = 1$, equations (11) and (2) are completely equivalent to the equations of laminar incompressible flow past a flat plate at zero incidence, or of a similar flow in a jet. Several well-known examples of jet flow are directly applicable.

Vertical mixing layer

The boundary conditions (12), illustrated in figure 1, correspond to the problem solved by Görtler (1942) for the laminar mixing of two uniform streams of incompressible fluid (see also Pai 1954). Following Görtler, one can fix the zero point of y by putting $u(x, 0) = \frac{1}{2}(U_1 + U_0)$, and obtain a series solution in powers of $(U_1 - U_0)/(U_1 + U_0)$, the coefficients of which are evaluated by numerical integration. The first two terms of Görtler's series give

$$u = U_0 + \frac{k_0 g\alpha}{\nu_0}\frac{T - T_0}{T_0} \approx \tfrac{1}{2}(U_1 + U_0)\left\{1 - \frac{U_1 - U_0}{U_1 + U_0}\operatorname{erf}\xi_1\right\}, \tag{18}$$

where

$$\operatorname{erf}\xi_1 = 2\pi^{-\frac{1}{2}}\int_0^{\xi_1} e^{-w^2}\,dw \quad \text{and} \quad \xi_1 = \left(\frac{U_1 + U_0}{8\kappa x}\right)^{\frac{1}{2}} y.$$

This approximate result is valid if $(U_1 - U_0)/(U_1 + U_0)$ is small.

Convection from a line source

Suppose that an unbounded porous medium, saturated with a fluid of temperature T_0 at rest under gravity, contains a horizontal line source of heat, of strength Q erg/cm sec. The origin of co-ordinates is taken at the line source, with the (x, y)-plane normal to it, the x-axis being directed vertically upwards.

Equations (11) and (2) are applicable, with $\sigma = 1$. For the boundary conditions, $\partial u/\partial y = v = 0$ at $y = 0$ by symmetry, while $u \to 0$ as $|y| \to \infty$. Further, since the system is in a steady state, the total vertical heat flux per unit length of source, at any given value of $x > 0$, must be equal to the source value.

$$Q = \int_{-\infty}^{\infty} Jc\rho(T - T_0)\,u^*\,dy = Jc\rho_0 T_0 \int_{-\infty}^{\infty} u(T - T_0)/T_0\,dy,$$

where the symbol J denotes the mechanical equivalent of heat. If use is made of (8), the following expression for 'kinematic heat flux' Q' is obtained:

$$Q' = \frac{k_0 g\alpha}{\nu_0} \frac{Q}{Jc\rho_0 T_0} = \int_{-\infty}^{\infty} u^2 dy. \tag{19}$$

Thus the problem is equivalent to that of the plane laminar incompressible momentum jet, solved by Schlichting (1933) and Bickley (1937) using boundary-layer theory. The similarity solution, quoted by Schlichting (1960), is

$$\left.\begin{aligned} u &= \tfrac{2}{3}(\tfrac{9}{16})^{\frac{2}{3}} (Q'^2/\kappa x)^{\frac{1}{3}} \operatorname{sech}^2 \xi, \\ v &= \tfrac{2}{3}(\tfrac{9}{16})^{\frac{1}{3}} (Q'\kappa/x^2)^{\frac{1}{3}} (2\xi \operatorname{sech}^2 \xi - \tanh \xi), \\ \text{where} \quad \xi &= \tfrac{1}{3}(\tfrac{9}{16})^{\frac{1}{3}} (Q'/\kappa^2 x^2)^{\frac{1}{3}} y, \end{aligned}\right\} \tag{20}$$

and the boundary-layer theory is valid provided that $Q'x/\kappa^2$ is large. For the total rate of fluid mass flow M across any horizontal section of the convection column,

$$M = \int_{-\infty}^{\infty} \rho u^* dy = \rho_0 \int_{-\infty}^{\infty} u\, dy = 4(\tfrac{9}{16})^{\frac{1}{3}} \rho_0 (Q'\kappa x)^{\frac{1}{3}}. \tag{21}$$

Convection from a point source

For the axially-symmetric flow arising from a point source of heat, the equation of continuity (2) is replaced by

$$\partial(yu)/\partial x + \partial(yv)/\partial y = 0,$$

where y is now the distance from the vertical x-axis, and the right-hand side of (11) is replaced by $\kappa y^{-1} \partial\{y\, \partial(\sigma u)/\partial y\}/\partial y$. It can easily be shown that the solution for the case $\sigma = 1$ is equivalent to the boundary-layer solution for the circular laminar incompressible jet (Schlichting 1933, 1960).

4. Experiments using a Hele–Shaw cell

The theory of Hele–Shaw flow of a homogeneous fluid has been summarized by Lamb (1932, § 330). If rectangular co-ordinates are taken in the plane of a cell sloping at an angle β to the horizontal, with the x-axis directed *down* the line of greatest slope, the fluid velocity averaged across the space between the plates at a given point is

$$(u, v) = (h^2/12\mu)\, (\partial/\partial x, \partial/\partial y)\, (-P + g\rho x \sin\beta). \tag{22}$$

Here P is the pressure, ρ and μ are the constant density and viscosity, h is the spacing between the plates, and $g \sin\beta$ is the gravity component in the plane of the cell. Equation (22) corresponds to a two-dimensional flow of homogeneous incompressible fluid through a porous medium of permeability $k_h = h^2/12\mu$.

A brief discussion of Hele–Shaw flow involving non-homogeneous fluid has been given elsewhere (Wooding 1960), where it is assumed that, if the mean-velocity components are slowly-varying functions of x and y, then the equation of continuity (2) and equations of motion of the form (3) and (4) still hold. Further, it is stated that an equation analogous to (5) with $\kappa_l = \kappa_t = \text{const.} = \kappa$ applies for the mass transport in the Hele–Shaw cell provided that $(2hw/\kappa)^2 \ll 210$, where w is the magnitude of the mean velocity.

Experimental method

A Hele–Shaw cell was constructed from two sheets of $\frac{1}{4}$ in. thick plate glass, each 30×20 cm, which was spaced at the corners by means of pieces of thin strip steel and clamped. In that way, a nearly uniform spacing of 0·351 mm was obtained between the glass sheets. The effective permeability of the cell was therefore $k_h = (0{\cdot}0351)^2/12 = 1{\cdot}03 \times 10^{-4}\,\mathrm{cm}^2$. The clamped assembly was mounted at an inclination β of 10° to the horizontal (figure 2(*a*)) in a glass aquarium tank filled with water. Except at the spacer locations, the interior of the cell was accessible to tank water at all points along the edges.

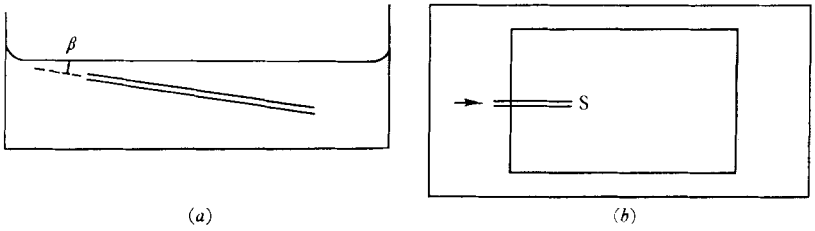

FIGURE 2. (*a*) Side view and (*b*) plan view of the experimental arrangement. A rectangular Hele–Shaw cell was mounted, at an angle β to the horizontal, in a glass aquarium tank filled with water; a capillary-tube source was located at S.

To provide a source of small dimensions inside the cell, a fine glass capillary tube was mounted at the upper end of the cell (figure 2(*b*)) to project into the space between the glass sheets to the source-point S. Fluid was supplied to the capillary tube from a reservoir which could be raised or lowered to vary the source strength. The source fluid was a potassium permanganate solution of density 1·0041 times that of water at the same temperature (about 18 °C). Thus the source fluid flowed downhill through the cell, in the direction of increasing x. At the given concentration of solution the molecular diffusivity κ of the potassium permanganate was about $0{\cdot}5 \times 10^{-5}\,\mathrm{cm}^2/\mathrm{sec}$ (Fürth & Ullman 1926), while the viscosity was only slightly above that of water—approximately 10^{-2} poise.

Plane jet from a virtual line source

This was formed in the experimental apparatus by using a very slow volume flow rate q of potassium permanganate solution—of order 0·1 c.c./h. The fluid mass flow rate M_s at the source and the solute mass flow rate Q were determined from the measured values of q and the solute concentration of the source fluid, i.e.

$$M_s = (\rho_1 q/2h)\,\mathrm{g/cm\,sec} \quad \text{and} \quad Q = \{(\rho_1 - \rho_0)/\rho_1\}\,M_s\,\mathrm{g/cm\,sec}, \tag{23}$$

where ρ_1 is the density of the source fluid and ρ_0 is the density of water.

Since the source supplied both fluid and dissolved material, instead of dissolved material alone as required by the theory of § 3, it was necessary to assume that the jet behaved as though it arose at a 'virtual line source' located at a distance l (say) behind the actual source. Thus the co-ordinates of the actual source were

$(l, 0)$, for an origin taken at the virtual source. The value of l was calculated from (21) and the expression for the 'kinematic flux of solute'

$$Q' = (k_h g \sin\beta/\mu)\, Q \tag{24}$$

analogous to (19). These expressions show that $l \propto M_s^2$.

In each of three experiments at different values of the source strength, the jet was 'started', and the distance z from the actual source to the leading edge of the advancing jet 'cap' (cf. Turner 1962) was measured as a function of time. The experimental parameters are given in table 1, while figures 3, (*a*) to (*d*), plate 1, shows four stages in the development of a jet for which

$$Q' = 5 \times 10^{-6}\,\mathrm{cm^3\,sec^{-2}}$$

approximately.

Expt no.	1	2	3
Source strength q (c.c./h)	0·08	0·12	0·14
Initial rate of descent (cm/h)	8·5	10	14·5
M_s (g/cm sec)	$0{\cdot}6_3 \times 10^{-3}$	$0{\cdot}9_5 \times 10^{-3}$	$1{\cdot}1_1 \times 10^{-3}$
Q (g/cm sec)	$2{\cdot}6 \times 10^{-6}$	$3{\cdot}9 \times 10^{-6}$	$4{\cdot}5_5 \times 10^{-6}$
Q' (cm³/sec²)	$4{\cdot}5_5 \times 10^{-6}$	$6{\cdot}8_5 \times 10^{-6}$	$8{\cdot}0 \times 10^{-6}$
l (cm)	0·3	0·7	$0{\cdot}9_5$

TABLE 1. Values of the parameters for three experiments on the convection column in a Hele–Shaw cell analogous to a plane 'starting jet'.

Now, as a test of the form of the similarity solution (20) for the convective flow from a line source, it is useful to assume that the shape and size of the jet cap relative to the steady jet behind it remains similar for all x, where x is taken to be the distance from the virtual source to the front of the steady jet column, excluding the cap (cf. Turner 1962, p. 362). This is fairly apparent from figure 3, where the measured width of the cap is found to increase as $x^{\frac{2}{3}}$ approximately. It then follows that the velocity of advance of the steady jet front should be a constant fraction of the steady-state axial flow rate (u_a say), i.e. if t denotes time,

$$dx/dt = Cu_a = C\tfrac{2}{3}(\tfrac{9}{16})^{\frac{2}{3}}\,(Q'/\kappa x)^{\frac{1}{3}}$$

from (20), where C is a numerical constant. Integration of this expression gives

$$x = \tfrac{3}{4}Q'^{\frac{1}{2}}\kappa^{-\frac{1}{2}}(\tfrac{8}{9}Ct)^{\frac{3}{4}}. \tag{25}$$

Let the distance from the virtual source to the leading edge of the jet cap be $x+b$ $(= z+l)$, where b is the length of the cap. From the similarity assumption, using (20) and (25),

$$b = \xi_c/\{\tfrac{1}{3}(\tfrac{9}{16})^{\frac{1}{3}}\,(Q'/\kappa^2x^2)^{\frac{1}{3}}\} = \xi_c(8C\kappa t)^{\frac{1}{2}}, \tag{26}$$

in which ξ_c is a second numerical constant. Equation (26) shows that the contribution b due to the jet cap, relative to the total measured length $z+l = x+b$, is

$$b/(x+b) = \{1 + (\tfrac{9}{16}[Q'x/\kappa^2])^{\frac{1}{3}}/3\xi_c\}^{-1}. \tag{27}$$

In § 3, it has been noted that $Q'x/\kappa^2$ must be large. From an inspection of figure 3 and from previous work (Turner 1962, p. 364) it appears that $\xi_c = O(1)$. If

$Q' = 5 \times 10^{-6}\,\mathrm{cm^3/sec^2}$ (cf. table 1), $\kappa = 0{\cdot}5 \times 10^{-5}\,\mathrm{cm^2/sec}$, and if $\xi_c \approx 1$, it is found that $b/(x+b) \approx 1/(1+16x^{\frac{1}{3}})$, where x is measured in cm; hence, as x becomes large, the measured quantity $z+l$ tends to x.

In figure 4, values of $10^{-3}(z+l)/Q'^{\frac{1}{4}}$ calculated from the experimental data are plotted against time. The points obtained from the three experiments apparently tend to the same limit—a straight line of slope $\frac{3}{4}$ in logarithmic co-ordinates—which agrees with (25) provided that $C \approx 0{\cdot}33$.

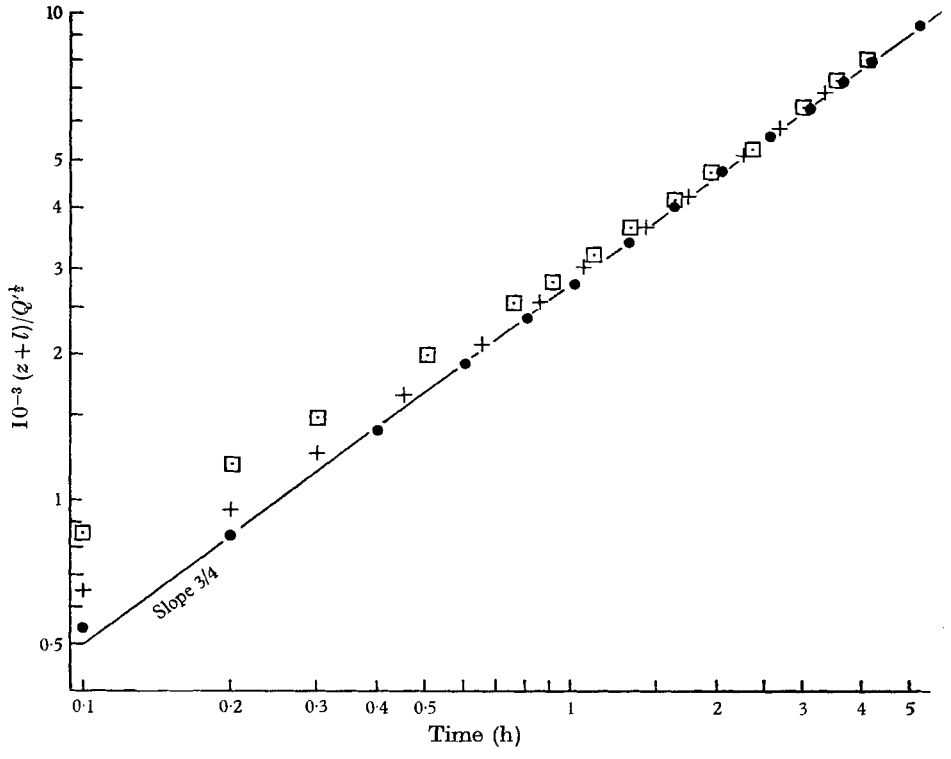

FIGURE 4. Values of $10^{-3}\,(z+l)/Q'^{\frac{1}{4}}$ *vs* elapsed time from table 1 for three experiments on the analogue of a plane jet. ●, Exp. 1; +, exp. 2; ⊡, exp. 3 (cf. table 1).

In the experimental work, it was found that an appreciable length of time was required for the jet front to pass beyond the local influence of the non-ideal source. The initial distribution of denser fluid about the source would resemble a circular bubble, of excess density $\rho_1 - \rho_0$, for which the rate of descent under gravity would be $\frac{1}{2}(k_h g \sin\beta/\mu)(\rho_1 - \rho_0)$ (Taylor & Saffman 1959). Substitution of the appropriate numerical values gives an initial rate of descent of about 13 cm/hour, in reasonable agreement with the observed values listed in table 1.

Broad jet

At sufficiently large values of the source strength, a 'broad jet' tending to a constant width was obtained (figure 5, plate 2), and the fluid rose a finite distance up the cell, forming a stagnation point above the source. Inside the jet, the fluid consisted of homogeneous potassium permanganate solution, while the

surrounding fluid (water) was at rest except for a slow inflow due to entrainment into the mixing layers.

If the mixing layers are neglected, the boundaries of the jet can be regarded as streamlines across which negligible pressure change occurs. The solution of the resulting potential problem can then be found as a limiting case of a problem discussed by Segedin & Miller (1962). Their equation for the boundary streamline is

$$\pi x/2d = \log\{\sec(\pi y/2d)\}, \tag{28}$$

where $2d$ is the limiting width of the jet, and the origin of co-ordinates is taken at the highest point of the jet (the stagnation point) with the x-axis directed down the slope of the cell. For the co-ordinates $(H, 0)$ of the source, they obtain

$$H/2d = \pi^{-1}\log 2 \approx 0{\cdot}2206. \tag{29}$$

Points calculated from (28) are plotted in figure 5, and show that the theoretical boundary shape is quite closely followed by the experimental jet. The results of measurements of the quantity $H/2d$ from the photographs of 11 experiments are given in table 2 for comparison with (29).

$2d$ (cm)	0·45	0·60	0·66	0·75	0·91	1·15
$H/2d$	0·24	0·20	0·21	0·21	0·19	0·20
$2d$ (cm)	1·27	1·65	2·34	3·05	3·48	Mean
$H/2d$	0·20	0·25	0·18	0·26	0·22	$0{\cdot}215 \pm 0{\cdot}025$

TABLE 2. Values of the ratio $H/2d$ obtained from 11 experiments at different values of the jet width $2d$. The theoretical value of 0·2206 given in (29) lies within the limits of experimental error.

Two Rayleigh numbers can be defined for the system as follows (cf. (16′) and (17′)):

$$\left.\begin{aligned} \lambda &= (k_h g \sin\beta/\kappa\mu)(\rho_1 - \rho_0) L \approx 1000L, \\ \text{and similarly,} \quad \lambda' &\approx 1000d^2/L \end{aligned}\right\} \tag{30}$$

if the numerical values appropriate to the experimental work are substituted. In (30), L is the distance along the mixing layer from the origin. In the experiments, measurements of the jet width were made at a level where $L \approx 3d$; thus the results shown in table 2 cover the ranges $700 < \lambda < 5000$ and $70 < \lambda' < 500$, and the conditions (16) and (17) are satisfied.

5. A geophysical application

Banwell (1957) has made use of borehole temperature measurements to plot isothermal maps for a number of cross-sections in the geothermal field at Wairakei, New Zealand. Tracings of isotherms from three of these diagrams (figures 7, 8 and 9 of Banwell's paper) have been reproduced in slightly modified form in

FIGURE 6. Isotherms for part of the Wairakei geothermal field (after Banwell 1957). (*a*) Horizontal cross-section 50 m below the datum level, (*b*) vertical cross-section intersecting the horizontal section (*a*) along line A, and (*c*) vertical cross-section intersecting the horizontal section along line B. The two vertical cross-sections intersect along line C. Temperature contours are labelled in °C.

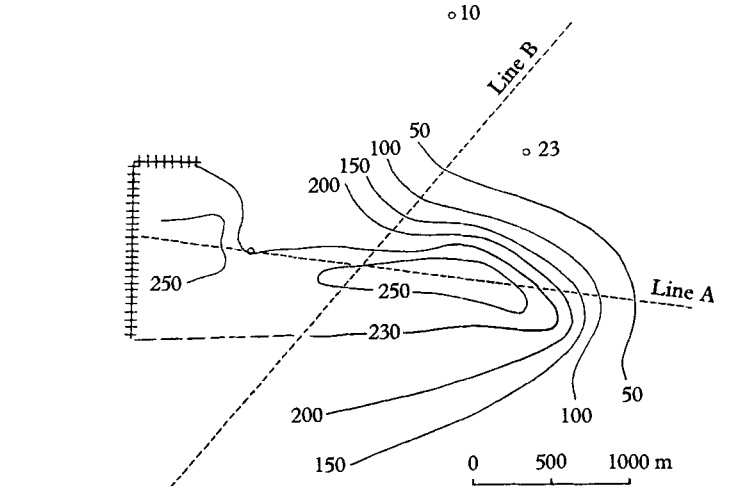

(*a*)

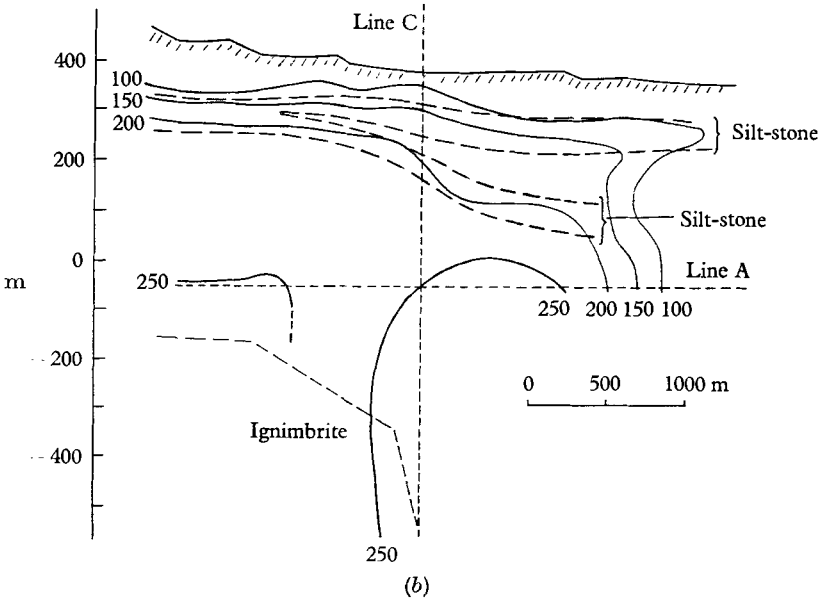

(*b*)

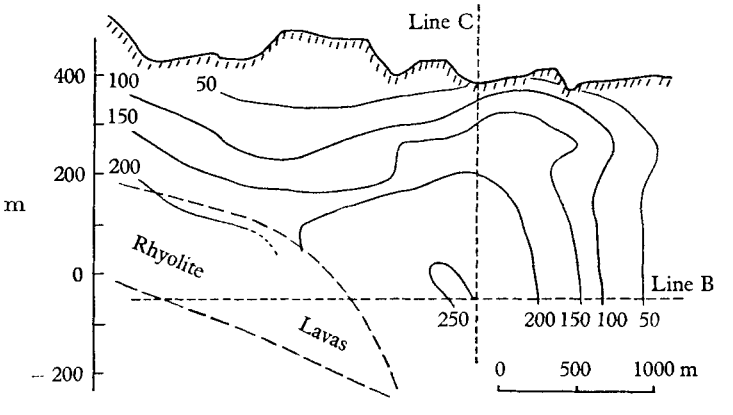

(*c*)

For legend see facing page.

figure 6. Figure 6(*a*) illustrates a horizontal cross-section at a depth of 50 m below the datum level (taking sea-level as datum), and also shows the lines of the two vertical cross-sections which are illustrated in figures 6 (*b*) and (*c*).

The vertical cross-sections indicate a region heated to temperatures in the vicinity of 250 °C, and separated from a region of normal temperature by a zone in which the isotherms are roughly vertical. It is interesting to consider the possibility that the flow pattern of the heated ground water possesses features of a vertical convection column, or 'hydrothermal jet', into which cold ground water is being entrained.

This postulated basic flow mechanism is complicated by variations in the geophysical properties of the system and the physical proximity of the ground surface. The principal disturbing features appear to be as follows:

(i) As the hot water approaches the ground surface, the reduction of pressure leads to rapid steam formation with consequent loss of temperature; this is indicated by closely spaced, roughly horizontal isotherms below the surface. The effect is concentrated at the silt-stone deposits from old lake beds (shown, for example, in figure 6 (*b*)) which are of relatively low permeability, and across which large pressure drops may be generated by the upward convective flow. The effect is not significant at depths greater than 400 m, i.e. below datum level. Since the pressure of saturated water vapour at 250 °C corresponds to the pressure exerted by a column of cold water about 400 m high, the pressure at greater depths is probably sufficiently great to maintain the geothermal fluid in liquid form.

(ii) The sideways 'bulge' in the isotherms above the vertical mixing layer in figure 6 (*b*) and (*c*) may arise as a result of horizontal outflow, close to the water-table, from the top of the vertical convection column.

(iii) Figure 6 (*c*) shows one edge of an extensive sheet of rhyolite—a product of an old volcanic lava flow. From drill-core samples, it has been shown that much of this deposit has not undergone chemical alteration due to hydrothermal action, and so must be impermeable; neither have conducting fissures been found (A. Steiner, pers. comm.).

(iv) The down-faulted ignimbrite shown in figure 6 (*b*) is also an impermeable volcanic material, but, in this case, fissures capable of conducting hydrothermal fluid may have been produced by faulting.

The deposits described in (iii) and (iv) may perhaps be regarded as impermeable blocks embedded in an extensive pumice breccia (fractured pumice) which exhibits a finite 'bulk permeability'; the total depth of volcanic debris is at least 3 km (Studt & Modriniak 1959).

Physical parameters

An estimate of the bulk permeability within the Wairakei geothermal region can be obtained from the measured discharge rate of heat at the ground surface (excluding geothermal bores) which is about $1{\cdot}6 \times 10^8$ g cal/sec relative to 15 °C (Thompson, Banwell, Dawson & Dickinson 1961). Consider the convective heat flow across the horizontal plane of figure 6 (*a*). It will be assumed that the predominant heat-transport mechanism is vertical convection, and that the

quantity of heat transported outside the very hot areas can be neglected; the 230 °C isotherm serves as a convenient boundary defining the limits of the hydrothermally-active zone (C. J. Banwell, pers. comm.). The rate of vertical heat transport across the plane is then approximately $(c\rho)_1 (T_1 - T_0) U_1 A$ g cal/sec, where A is the area bounded by the 230 °C isotherm and the suffix 1 indicates values of the parameters within that area. From (8),

$$U_1 = (k_1 g\alpha/\nu_1)(T_1 - T_0)/T_0 \text{ cm/sec}.$$

Now, taking $T_1 - T_0 = 225°$ gives $\alpha(T_1 - T_0)/T_0 \approx 0{\cdot}2$, $\nu_1 \approx 1{\cdot}4 \times 10^{-3}$ cm^2/sec and $(c\rho)_1 \approx 0{\cdot}9$. The area A is known with less accuracy, but the area bounded by the 230 °C isotherm and the cross-hatched lines in figure 6(*a*) is 2 km^2. A reasonable value for the total area would be about 5 km^2. Substituting these values gives

$$k_1 \approx 10^{-10} \text{ cm}^2 \quad \text{(i.e. } 0{\cdot}01 \text{ darcy)}$$

and

$$U_1 \approx 1{\cdot}5 \times 10^{-5} \text{ cm/sec}.$$

From these results, the total rate of upflow of water $\rho_1 U_1 A$ is about 600 kg/sec, which may be compared with the measured outflow of about 430 kg/sec at the surface (Thompson *et al.* 1961). Thus the values of k_1 and U_1 appear to be of the correct orders of magnitude.

Outside the heated region, the value of k may increase considerably, perhaps by one or more orders of magnitude (J. Healy and G. W. Grindley, pers. comm.). This effect could arise because chemical deposition occurs within the geothermally active region, leading to cementing of the fractured material.

Measurements of thermal diffusivity near the surface give a value of about 0·0025 cm^2/sec for saturated ground (Thompson *et al.* 1961). To allow for the effect of soil compaction, a value of $\kappa \approx 0{\cdot}003$ cm^2/sec will be chosen to apply at depths greater than 400 m, where it is assumed that little steam is present.

The steady-state mixing-layer model

For the calculation of temperature and flow rate within the postulated vertical mixing layer, it is convenient to use the von Mises equations (14) with boundary conditions (12), taking $U_0 = 0$. With the approximate values of U_1 and κ given above, the Péclet number based upon pore size is $O(10^{-2}s)$, where s is the length scale of the pores or small fissures. If s does not exceed the order of 100 cm, it is sufficiently accurate to take $\kappa_t = \kappa$ for the transverse diffusivity, as assumed previously.

The variation of kinematic viscosity of water with temperature can be represented approximately by the empirical formula (Wooding 1957)

$$\left.\begin{aligned} \nu/\nu_0 &= (1 + a\theta)^{-1}, \\ \text{where} \qquad \theta &= (T - T_0)/(T_1 - T_0) \quad \text{and} \quad a = (T_1 - T_0)/(T_0 - 260). \end{aligned}\right\} \tag{31}$$

However, since the variation of permeability with temperature is only known qualitatively, it is convenient to assume that k is a function of temperature alone, and to write for the quantity σ the one-parameter formula

$$\sigma = \frac{\nu}{k} \Big/ \frac{\nu_0}{k_0} = (1 + b\theta)^{-1}, \tag{31'}$$

where $b = a$ if the permeability is constant. Then the case $b = 0$ implies that $k \propto \nu$ (including the case of constant k and ν).

From (8), the equation of motion is

$$\sigma u = (k_0 g\alpha/\nu_0)(T - T_0)/T_0 = \sigma_1 U_1 \theta, \tag{32}$$

where $\sigma_1 = 1/(1+b)$. If a similarity solution involving the variable transformation

$$\eta = -\psi/(4\kappa U_1 x)^{\frac{1}{2}}$$

is assumed to exist, the partial differential equation in (14) becomes an ordinary equation; from (14),

$$\left.\begin{aligned} \frac{d}{d\eta}\left(\frac{1+b\theta}{1+b}\theta\frac{d\theta}{d\eta}\right) + 2\eta\frac{d\theta}{d\eta} = 0, \\ \left(\frac{U_1}{4\kappa x}\right)^{\frac{1}{2}} y = -\int\frac{(1+b)\,d\eta}{\theta(1+b\theta)}, \end{aligned}\right\} \tag{33}$$

after elimination of u and σ. (The form of (31′) is such that θ, or σu, becomes the most convenient dependent variable.) Since $U_0 = 0$, the stream-function ψ must tend to a limit as $y \to \infty$. Let the corresponding limit for the independent variable η be $-\eta_0$, where $\eta_0 > 0$. Then the boundary conditions upon (33) can be written

$$\theta(-\eta_0) = 0, \quad \theta(\infty) = 1,$$

together with an additional requirement that the solution of (33) should be of the correct asymptotic form as $y \to \infty$, or $\eta \to -\eta_0$.

In the neighbourhood of $\eta = -\eta_0$, a series expansion of Blasius type for θ in powers of $\eta + \eta_0$ with leading term $2\eta_0(1+b)(\eta+\eta_0)$ is found to be appropriate, since this gives the correct asymptotic expression

$$\theta \sim \exp\{-2\eta_0(U_1/4\kappa x)^{\frac{1}{2}} y\} \tag{34}$$

as $y \to \infty$. Physically, while θ and hence the vertical component of the flow rate vanish exponentially, a slow horizontal entrainment inflow v_e persists, balancing the effect of transverse thermal diffusion. From the definition of η, it is readily found that

$$v_e \sim -\eta_0(\kappa U_1/x)^{\frac{1}{2}}. \tag{35}$$

When $\eta \to \infty$ $(y \to -\infty)$, the asymptotic solution is

$$\left.\begin{aligned} 1 - \theta \sim \operatorname{erfc}\eta = \int_\eta^\infty e^{-\eta^2}\,d\eta \\ \text{and} \qquad (U_1/4\kappa x)^{\frac{1}{2}} y \sim -\eta. \end{aligned}\right\} \tag{36}$$

The series expansion near $\eta = -\eta_0$ is found to be of little value when b is large. However, equations (33) can be solved numerically, treating η_0 as a constant to be determined; it is found useful to introduce the transformations

$$c = b(1+b)\eta_0^2, \quad \Theta = \theta/(1+b)\eta_0^2 \quad \text{and} \quad X = (\eta+\eta_0)/\eta_0,$$

so that the series becomes

$$\Theta = 2X - (1+4c)\frac{X^2}{2!} + \tfrac{1}{6}(1+4c)(1+36c)\frac{X^3}{3!} - \ldots, \tag{37}$$

which is valid as $X \to 0$. For a suitably chosen value of c, the transformed version of the differential equation in (33) is then integrated by the Runge–Kutta method, starting from a small value of X and using (37) to provide starting values of Θ and $d\Theta/dX$. The step length of the numerical process is initially taken very small, but is increased as X increases. At large X, the solution tends to the limit $\Theta(\infty) = 1/\eta_0^2$, thus determining η_0. The integral in (33) is also evaluated numerically.

In figure 7, values of η_0 are plotted as a function of b. When $b \gg 1$, the flow is dominated by the fact that water at the low temperature T_0 is much more viscous than water at the high temperature T_1. The parameter η_0 has a low value in (34)

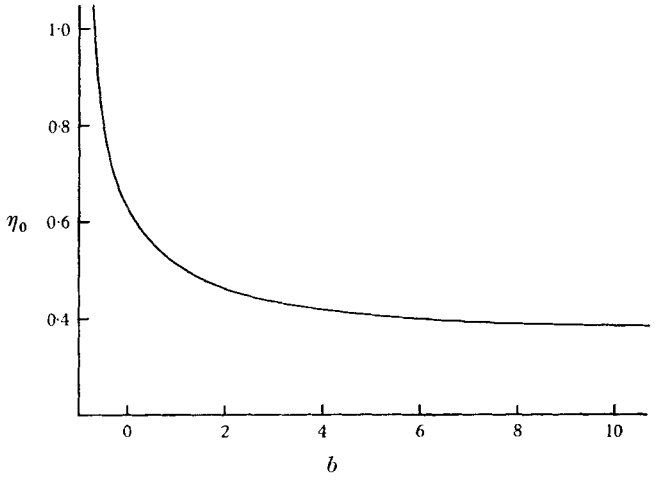

FIGURE 7. Values of η_0 for different values of the parameter b, from the numerical solution of the mixing-layer equations (33).

and (35), so that the mixing layer is wide. When b is small, the greater permeability in the region at temperature T_0 largely counteracts the effect of the viscosity variation ($k/k_0 \approx \nu/\nu_0$) and the entrainment flow v_e is increased, thus reducing the width of the mixing zone.

Comparison with temperature measurements

Measurements have been made of temperature *vs* distance along the lines of intersection, A and B, of the horizontal cross-section in figure 6(*a*) with the vertical cross-sections of 6(*b*) and (*c*), and values of $\theta = (T - T_0)/(T_1 - T_0)$ calculated from these measurements are plotted in figure 8. Here it is assumed that the upper and lower temperature limits are 240° and 10 °C. Since the temperature distribution in the region above 200 °C is rather irregular, the upper limit is not well defined. However, a reliable lower limit can be determined from temperature measurements in 'cold' bore-holes outside the hydrothermal region; the closest, labelled '10' in figure 6(*a*), registers temperatures between 10° and 11 °C from the surface to the maximum depth of about 250 m (G. E. K. Thompson, pers. comm.).

It is apparent from figure 8 that the two sets of temperature measurements are in very good agreement except at temperatures above 200 °C. This agreement may be fortuitous since, as indicated in figure 6(*a*), the isotherms intersected by line A are convex, while the isotherms intersected by line B are concave, towards the outer cold region. A two-dimensional theory should apply only roughly to the geophysical data.

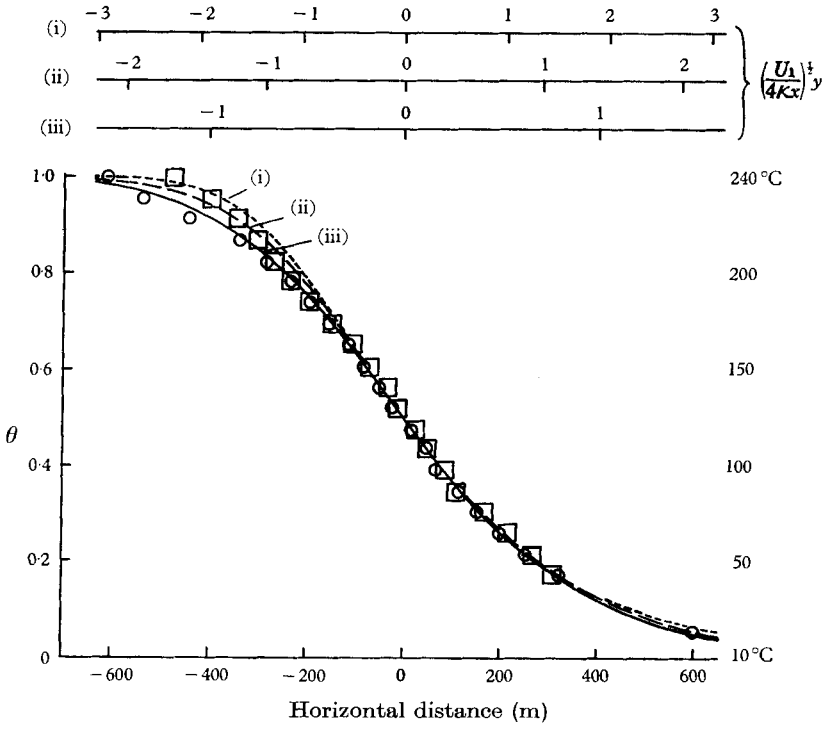

FIGURE 8. Values of $\theta = (T - T_0)/(T_1 - T_0)$ plotted *vs* horizontal distance from Banwell's (1957) results in figure 6; □, values of θ along line A; ○, values of θ along line B. Also shown are the θ-profiles calculated numerically from (33) for models (i), (ii), and (iii) described in the text. The arbitrary origins of the horizontal scales have been adjusted to coincide at the point for which $\theta = 0{\cdot}5$.

Three mixing-layer models, calculated from (33) with parameter values (i) $b = 10$, (ii) $b = 0$ and (iii) $b = -0{\cdot}677$, have been fitted graphically to the data in figure 8. Since the numerical values for T_1 and T_0 give $a = 10$ in formula (31) for the viscosity ratio, model (i) represents a porous medium of constant permeability, while model (ii) represents a medium in which the permeability is proportional to the kinematic viscosity; the maximum permeability contrast is $k_0/k_1 = 11$. In model (iii), $k_0/k_1 \approx 30$. In spite of these considerable physical differences, the three curves shown in figure 8 are remarkably similar in form. There is an indication that models (ii) and (iii) are better-fitted to the data than is model (i), implying that a decrease of permeability occurs as the heated region is approached.

From the graphical fitting process used in figure 8, the scale unit $(4\kappa x/U_1)^{\frac{1}{2}}$ of each mixing-layer model is known in terms of actual physical distance. Then, if use is made of the numerical values previously assigned to the various physical parameters, the depth x $(= L)$ to the virtual source can be calculated. These results, together with values of entrainment flow v_e calculated from (35), and the magnitudes of the Rayleigh numbers estimated from (16′) and (17′), are given in table 3. In the estimate of λ', the horizontal scale width $2d$ of the assumed broad-jet model is taken to be about 1 km, based upon an inspection of figure 6(*a*). It will be seen that the conditions (16) and (17) of § 2 are satisfied by λ and λ'; also, from figure 8, it is evident that the broad-jet model provides a satisfactory fit to the geophysical data. (The plane-jet model (20) is found to provide a much poorer fit.)

Model	(i)	(ii)	(iii)
Permeability ratio k_0/k_1	1	11	30
Depth to virtual source: 10^{-5} L (km)	5·5	10	20
Entrainment flow rate: $-v_e$ (cm/sec)	$1{\cdot}1 \times 10^{-7}$	$1{\cdot}3 \times 10^{-7}$	$1{\cdot}4 \times 10^{-7}$
Rayleigh numbers λ	$> 10^3$	$> 10^3$	$> 10^3$
Rayleigh numbers λ'	$O(10)$	$O(10)$	$O(10)$

TABLE 3. Parameter values deduced for the Wairakei geothermal field using the three different mixing-layer models (i) $b = 10$ (constant permeability), (ii) $b = 0$ (permeability proportional to kinematic viscosity) and (iii) $b = -0{\cdot}677$ (permeability varying more rapidly than kinematic viscosity).

As the properties of the actual source of hot fluid probably depart considerably from those of the assumed ideal source, the calculated values of L may be a great deal larger than the actual depth of the source. The actual depth is probably of the same order of magnitude as the depth of the volcanic deposits, found by Studt & Modriniak to be of the order of 3 km or greater.

The time required for a given fluid particle to pass through the hydrothermal system is $O(\epsilon L/U_1)$, where the porosity $\epsilon = O(10^{-1})$. From the numerical values for the three mixing-layer models, the transit time probably lies between 200 and 1000 years. This is in agreement with isotopic evidence (C. J. Banwell, pers. comm.) which indicates that the geothermal water has been out of contact with the atmosphere for more than 50 years, but less than 10^4 years.

It has been tacitly assumed in the above discussion that the hydrothermal system is in a steady, or quasi-steady, state. A simple calculation shows that the time constant for the mixing layer is $O(L^2\delta^2/\kappa) = O(L/U_1)$ from (15)—in this case, a few thousand years. From petrological evidence (A. Steiner and G. W. Grindley, pers. comm.), it is known that hydrothermal activity was present at Wairakei more than 10^5 years ago, but it is not known whether the system has fluctuated considerably during that long period, or whether it has remained relatively steady.

As a check upon the inflow to the postulated convective system, it has been noted that bore-holes drilled in cold areas at distances of order 10 km from Wairakei show an absence of vertical thermal gradient (F. E. Studt, pers. comm.).

This has been interpreted as a result of downflow of surface water, due to drainage into the hydrothermal region, and furnishes the best available evidence that the country surrounding the Wairakei system is permeable to ground water. The natural heat outflow from the earth is $O(10^{-6})$ cal/cm^2 sec, and this usually gives rise to temperature gradients of order 30 °C/km (Jeffreys 1959, p. 298). If that heat flow is imagined to arise from a source at a temperature of 1000 °C at a depth of 30 km, a ground-water downflow rate of 10^{-7} cm/sec would be sufficient to reduce the surface vertical gradient to less than 1/1000 of its normal value. The temperature gradient would then not be detectable. It is interesting to note, from the values of v_e in table 3, that the inflow due to entrainment into the hydrothermal jet could lead to a surface downflow approaching that order of magnitude.

The author wishes to acknowledge the benefit of valuable discussions with Messrs C. J. Banwell, G. W. Grindley, F. E. Studt, A. Steiner, J. Healy and G. E. K. Thompson. Special thanks are due to Mr Banwell for permission to reproduce diagrams from a published paper, and to make use of certain unpublished data. Numerical calculations were performed upon the IBM computer at the Treasury, Wellington, with the assistance of Mr E. W. Jones.

REFERENCES

BANWELL, C. J. 1957 *Proc. ASME*, **79**, 255.

BICKLEY, W. G. 1937 *Phil. Mag.* (7), **23**, 727.

FÜRTH, R. & ULLMAN, E. 1926 *Kolloidschr.* **41**, 307.

GÖRTLER, H. 1942 *Z. angew. Math. Mech.* **22**, 244.

JEFFREYS, Sir HAROLD 1959 *The Earth*, 4th ed. Cambridge University Press.

LAMB, H. 1932 *Hydrodynamics*. Cambridge University Press.

MISES, R. VON 1927 *Z. angew. Math. Mech.* **7**, 425.

PAI, S.-I. 1954 *Fluid Dynamics of Jets*. New York: Van Nostrand.

SAFFMAN, P. G. 1960 *J. Fluid Mech.* **7**, 194.

SCHLICHTING, H. 1933 *Z. angew. Math. Mech.* **13**, 260.

SCHLICHTING, H. 1960 *Boundary Layer Theory*, 4th ed. New York: McGraw-Hill.

SEGEDIN, C. M. & MILLER, J. B. 1962 *N. Z. J. Sci.* **5**, 43.

STUDT, F. E. & MODRINIAK, N. 1959 *N. Z. J. Geol. Geophys.* **2**, 654.

TAYLOR, Sir GEOFFREY & SAFFMAN, P. G. 1959 *Quart. J. Mech. Appl. Math.* **12**, 265.

THOMPSON, G. E. K., BANWELL, C. J., DAWSON, G. B. & DICKINSON, D. J. 1961 *U.N. Conference on New Sources of Energy*, Paper no. E/CONF. 35/G/54.

TURNER, J. S. 1962 *J. Fluid Mech.* **13**, 356.

WOODING, R. A. 1957 *J. Fluid Mech.* **2**, 273.

WOODING, R. A. 1960 *J. Fluid Mech.* **7**, 501.

YIH, C.-S. 1961 *J. Fluid Mech.* **10**, 133.

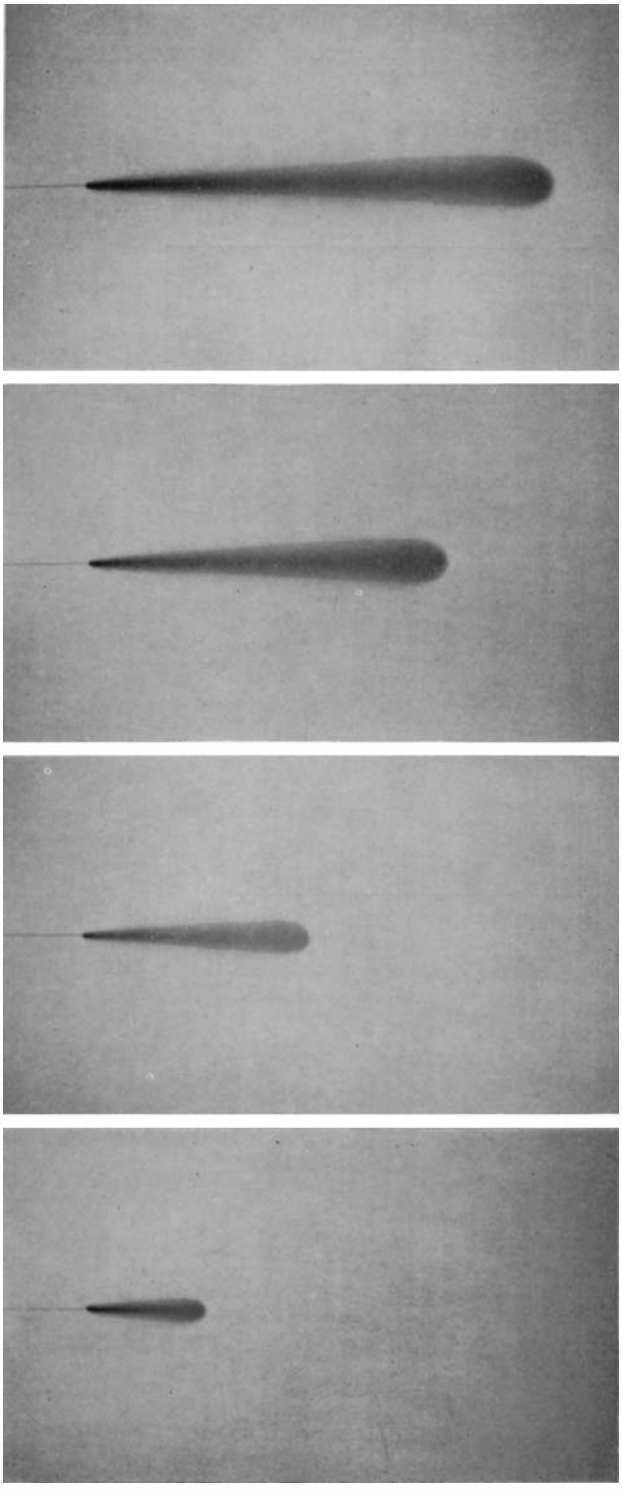

(*a*) (*b*) (*c*) (*d*)

FIGURE 3. Convection column of potassium permanganate solution in a Hele-Shaw cell, analogous to a plane jet, for distances from the source to the leading edge of the column of (*a*) 5 cm, (*b*) 10 cm, (*c*) 15 cm and (*d*) 20 cm.

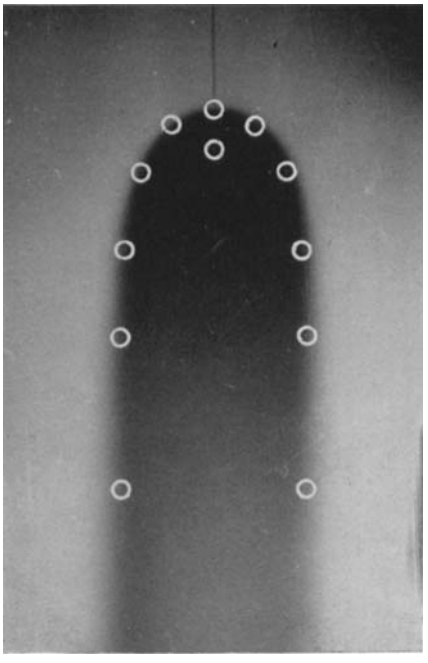

FIGURE 5. Analogue of a broad jet produced in a Hele–Shaw cell, with points calculated from (28) for the bounding streamline on the assumption that the effect of mixing layers can be neglected.